Photosynth Res (2013) 117:401–412
DOI 10.1007/s11120-013-9875-5

REGULAR PAPER

Efficiency of photosynthetic water oxidation at ambient and depleted levels of inorganic carbon

Dmitriy Shevela · Birgit Nöring · Sergey Koroidov · Tatiana Shutova · Göran Samuelsson · Johannes Messinger

Received: 23 March 2013 / Accepted: 20 June 2013 / Published online: 5 July 2013

Abstract Over 40 years ago, Joliot et al. (Photochem Photobiol 10:309–329, 1969) designed and employed an elegant and highly sensitive electrochemical technique capable of measuring O_2 evolved by photosystem II (PSII) in response to trains of single turn-over light flashes. The measurement and analysis of flash-induced oxygen evolution patterns (FIOPs) has since proven to be a powerful method for probing the turnover efficiency of PSII. Stemler et al. (Proc Natl Acad Sci USA 71(12):4679–4683, 1974), in Govindjee's lab, were the first to study the effect of "bicarbonate" on FIOPs by adding the competitive inhibitor acetate. Here, we extend this earlier work by performing FIOPs experiments at various, strictly controlled inorganic carbon (C_i) levels without addition of any inhibitors. For this, we placed a Joliot-type bare platinum electrode inside a N_2-filled glove-box (containing 10–20 ppm CO_2) and reduced the C_i concentration simply by washing the samples in C_i-depleted media. FIOPs of spinach thylakoids were recorded either at 20-times reduced levels of C_i or at ambient C_i conditions (390 ppm CO_2). Numerical analysis of the FIOPs within an extended Kok model reveals that under C_i-depleted conditions the miss probability is discernibly larger (by 2–3 %) than at ambient conditions, and that the addition of 5 mM HCO_3^- to the C_i-depleted thylakoids largely restores the original miss parameter. Since a "mild" C_i-depletion procedure was employed, we discuss our data with respect to a possible function of free or weakly bound HCO_3^- at the water-splitting side of PSII.

Keywords Flash-induced oxygen evolution patterns · S states · An extended Kok model · Hydrogen carbonate (bicarbonate) · Photosynthetic water oxidation

Abbreviations

α	Miss parameter
β	Double hit parameter
C_i	Inorganic carbon (HCO_3^-, CO_2, CO_3^{2-})
C_i^-	Inorganic carbon depleted
C_i^+	Containing ambient level of inorganic carbon
FIOP	Flash-induced oxygen evolution pattern
MIMS	Membrane-inlet mass spectrometry
PSII	Photosystem II
OEC	Oxygen-evolving complex
S_i states	Oxidation states of the OEC, where i is the number of stored oxidizing equivalents

Introduction

Oxygenic photosynthesis is a fundamental biological process by which higher plants, algae, and cyanobacteria reduce atmospheric CO_2 to energy-rich carbohydrates using the electrons extracted from water during oxidative water-splitting. Photosynthetic water-splitting takes place in the oxygen-evolving complex (OEC) of photosystem II (PSII), a large pigment-binding protein complex found in

D. Shevela (✉) · S. Koroidov · J. Messinger (✉)
Department of Chemistry, Chemical Biological Centre,
University of Umeå, 90187 Umeå, Sweden
e-mail: dmitriy.shevela@chem.umu.se

J. Messinger
e-mail: johannes.messinger@chem.umu.se

D. Shevela · B. Nöring · J. Messinger
Max Planck Institute for Chemical Energy Conversion,
45470 Mülheim, Germany

T. Shutova · G. Samuelsson
Department of Plant Physiology, Umeå Plant Science Centre,
Umeå University, 90187 Umeå, Sweden

all oxygen-evolving organisms (Wydrzynski and Satoh 2005; Govindjee et al. 2010; Kouril et al. 2012). The OEC contains a μ-oxo bridged tetra-manganese calcium (Mn_4CaO_5) cluster (Yano et al. 2006; Umena et al. 2011) that is capable of step-wise oxidation of water into four protons, four electrons, and molecular oxygen (Messinger and Renger 2008; Dau et al. 2012; Cox and Messinger 2013). The energy for this is provided by light-induced charge separation within the chlorophyll-containing reaction center of PSII (Renger and Holzwarth 2005; Renger 2010).

The current understanding of the mechanism of photosynthetic water oxidation originates from the classic measurements of flash-induced oxygen evolution patterns (FIOPs) performed by Joliot et al. (1969). By illuminating dark-adapted algae and chloroplasts with a train of short saturating (single turn-over) light flashes and by employing a specially designed highly sensitive rapid-response polarograph for O_2 detection, Joliot et al. (1969) observed that: (i) no O_2 was evolved in response to the 1st flash; (ii) a small O_2 yield was induced by the 2nd flash; (iii) the most pronounced maximum of O_2 yield occurred after the 3rd flash; (iv) subsequent flashes induced an oscillating pattern of O_2 evolution with a maximum on every 4th flash (i.e., in the 7th, 11th, 15th,…); and (v) this period-four oscillation gradually disappeared after several cycles. Figure 1a illustrates this notable FIOP in its original version as obtained by Joliot et al. (1969) (for historical review, see Joliot 2003). On the basis of these observations, Kok and coworkers developed a kinetic model (also known as *"Kok model"* or *"Kok cycle"*) demonstrating a four-electron chemistry of water oxidation and O_2 production by the OEC (see Kok et al. 1970 and, for an early discussion of this and other models, see Mar and Govindjee 1972). According to the Kok model, the OEC cycles through five redox intermediates during water oxidation, which were termed S_i states ($i = 0,\ldots,4$), where i signifies the number of stored oxidizing equivalents (see Fig. 1b). Upon accumulation of four oxidizing equivalents, the highly reactive S_4 state decays into the S_0 state while two H_2O molecules are oxidized to O_2.

In well dark-adapted samples, almost all PSII centers are in the "dark-stable" S_1 state (that is why the first maximum of O_2 evolution is observed upon the 3rd flash). This is due to the deactivation of the metastable S_0, S_2, and S_3 states to S_1 via different pathways that involve a redox active tyrosine residue (Y_D) and the reduced acceptor side quinones (Diner 1977; Vermaas et al. 1984; Nugent et al. 1987; Styring and Rutherford 1987; Vass et al. 1990a; Messinger and Renger 1993; Isgandarova et al. 2003). In order to explain the observed disappearance of the O_2 oscillation patterns with increasing number of flashes, the S_i state turnovers are suggested to be coupled to the so-called "miss" and "double hit" probabilities (Kok et al. 1970; Forbush et al. 1971). The miss probability (α) accounts for the failed advancement of the S_i cycle to the next S state (i.e., $S_i \rightarrow S_i$ transitions) upon flash excitation. The "misses" were suggested to be dependent on all redox equilibria and kinetics of both the donor and acceptor side of PSII, as well as on pH and temperature; thus, it represents a very sensitive probe for the changes in the turnover efficiency of PSII under various conditions and sample treatments (see reviews by Shinkarev 2005; Messinger and Renger 2008; Renger and Hanssum 2009, and references therein). The classical Kok model assumed that the miss parameter is S_i state and flash number independent. However, there is experimental data indicating that α-values are dependent on the redox state S_i of the OEC (Renger and Hanssum 1988; Shinkarev and Wraight 1993; de Wijn and van Gorkom 2002; Isgandarova et al. 2003; Han et al. 2012; Suzuki et al. 2012). Since under most circumstances, the kinetics of electron transfer on the acceptor side are limiting for the S-state advancement (Fromme et al. 1987; Ananyev and Dismukes 2005; Shevela and Messinger 2012) the double hits (i.e., $S_i \rightarrow S_{i+2}$ transitions) reflect mostly events on the electron-acceptor side (namely on Q_A and Q_B, the primary and secondary plastoquinone electron acceptors of PSII). The magnitude of the double hits is affected by the FWHM-flash profile (Kok et al. 1970; Jursinic 1981; Messinger et al. 1993). In addition to miss and double hit parameters our extended Kok models include other factors that can affect FIOPs (Hillier and Messinger 2005; Messinger and Renger 2008). Among them, for instance, there is a correction factor that accounts for a change of the number of active PSII centers during the flash train (Kebekus et al. 1995; Messinger et al. 1997), and back reactions of S_2 and S_3 states with Y_D during the dark time between flashes (Vass et al. 1990a; Messinger and Renger 1993; Isgandarova et al. 2003).

Despite numerous reports about the requirement of hydrogen carbonate ("bicarbonate"; HCO_3^-) and other inorganic carbon (C_i) species (CO_2, CO_3^{2-}) for optimal stability and/or activity of the OEC of PSII, its role—if any—in photosynthetic water-splitting chemistry remains highly controversial. The first report by Warburg and Krippahl (1958) on the "*bicarbonate effect*" on the electron flow in PSII triggered many subsequent studies by other research groups (for recent reviews, see McConnell et al. 2012; Shevela et al. 2012). Since then, two sites of HCO_3^- action were explored within PSII. In 1975, a pioneering work by Wydrzynski and Govindjee (1975) provided a strong evidence for the participation of HCO_3^- ions in the electron transfer on the acceptor side of PSII (Wydrzynski and Govindjee 1975). Numerous subsequent experiments showed that this *electron-acceptor side* HCO_3^- facilitates the reduction of Q_B and participates in

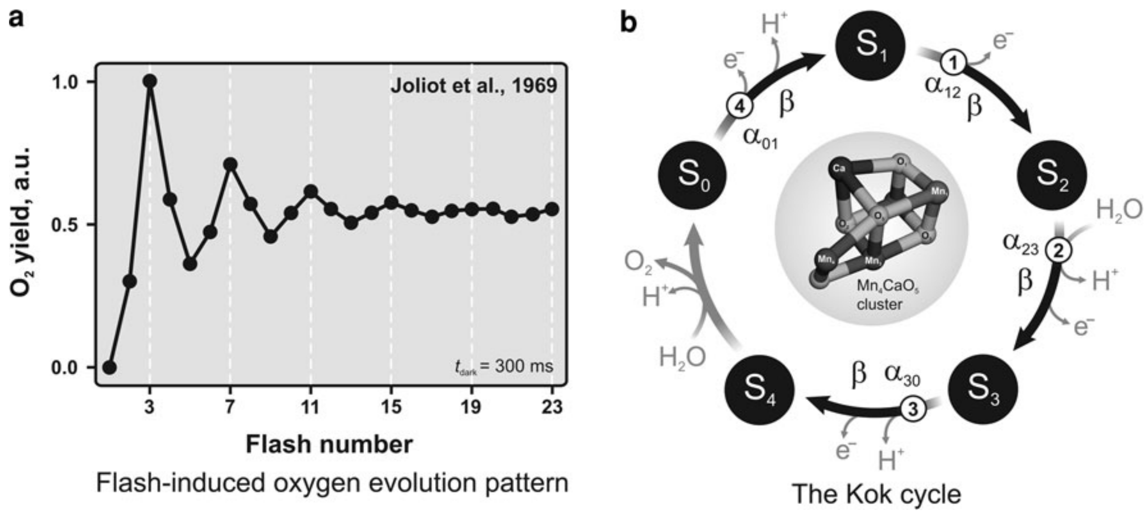

Fig. 1 Classical flash-induced oxygen evolution pattern (FIOP) as was first obtained by Joliot et al. (1969) in dark-adapted spinach chloroplasts upon illumination with a series of single saturating light flashes (separated with dark time of 300 ms) at pH 7.9 and 20 °C (**a**), and the Kok cycle that describes this phenomenon and represent the reaction scheme of photosynthetic water oxidation and oxygen evolution (**b**). **a** is modified and adapted from Joliot et al. (1969). In **b**, light-induced S-state transitions of the Kok cycle are shown by *black arrows* and the number of light flashes required for a certain transitions are indicated by *numbers in circles* on the *arrows*, assuming that in the dark, the Mn_4CaO_5 cluster (shown in the *center of the cycle*) is mostly in the S_1 state. *Gray arrow* between S_4 and S_0 states indicates the transition that does not require light. Note that one water molecule is entering the cycle on the $S_2 \rightarrow S_3$ transition, and another on the $S_4 \rightarrow S_0$ transition. For the original version of the Kok cycle, see Kok et al. (1970) and Forbush et al. (1971). The structural model of the Mn_4CaO_5 cluster is as derived from the recent PSII crystal structure at a 1.9 Å resolution (Umena et al. 2011). For explanation of all other symbols in the Kok cycle, see text

protonation reactions near the Q_B-binding site (Van Rensen et al. 1999; Van Rensen 2002; McConnell et al. 2012; Shevela et al. 2012). Another site for "bicarbonate" action is thought to be the *electron-donor side* of PSII, where HCO_3^- ions may be required for optimal functionality and stability of the OEC, and for the photo-induced assembly of the inorganic core of the OEC (Stemler 2002; Van Rensen and Klimov 2005; Dasgupta et al. 2008). HCO_3^- binding to the non-heme Fe between two quinones Q_A and Q_B on the acceptor side of PSII was recently confirmed by X-ray crystallography studies of PSII (Ferreira et al. 2004; Guskov et al. 2010; Umena et al. 2011). In contrast, the site of interaction of HCO_3^- on the donor side is not obvious. Based on recent X-ray crystallography (Umena et al. 2011), mass spectrometry (Shevela et al. 2008b; Ulas et al. 2008), and FTIR spectroscopy (Aoyama et al. 2008) studies, HCO_3^- does not bind tightly at or near the Mn_4CaO_5 cluster. At the same time, the possibility for a weakly bound, mobile, and rapidly exchanging HCO_3^- within the OEC cannot be excluded. Thus, for instance, HCO_3^- was recently proposed to act as an acceptor of protons produced during water-splitting (see Fig. 1b) (Villarejo et al. 2002; Ananyev et al. 2005; Shutova et al. 2008; Pobeguts et al. 2010; Ulas and Brudvig 2010).

In case of the participation of mobile or weakly bound HCO_3^- ions in the water-oxidizing reactions of the OEC, their removal should impair the efficiency of the S_i state transition. In this regard, important information on the turnover efficiency of PSII before and after the C_i-depletions can be obtained from the FIOPs measurements. The first results revealing the effect of the C_i-depletion on FIOPs were obtained in Govindjee's group by Stemler et al. (1974). In that report, authors observed strong damping of FIOPs in HCO_3^--depleted chloroplasts, indicating impaired turnover efficiency of PSII upon removal of HCO_3^-. In that and numerous subsequent FIOPs experiments effect of HCO_3^- on PSII was studied by addition of chemical analogs of HCO_3^-, such as acetate or formate (combined with low pH treatments) to photosynthetic samples (Stemler and Govindjee 1973; Stemler et al. 1974; Stemler 1980, 1982; Jursinic and Stemler 1982, 1984; Vermaas et al. 1984; Mende and Wiessner 1985; Stemler and Lavergne 1997; Shevela et al. 2007). However, since later the above-mentioned anions were shown to remove a tightly bound HCO_3^- from the acceptor side of PSII (Govindjee et al. 1991, 1997; Shevela et al. 2008a, b; Ulas et al. 2008), such C_i depletion procedure is not suitable for elucidation of the possible participation of weakly bound HCO_3^- in the water-splitting reactions of PSII. Therefore, for studies of the donor side "bicarbonate effects," a milder C_i-depletion method was developed, in which dilution and washing of the samples in C_i-depleted media is used to remove C_i from the samples, but not affecting HCO_3^- bound on the acceptor side of PSII (Klimov et al. 1995a, b).

Because of the chemical characteristics of the CO_2/HCO_3^- system, expressed by Eq. 1:

$$CO_2 + H_2O \leftrightarrow H_2CO_3 + H_2O \overset{pK_a}{\leftrightarrow} HCO_3^- + H_3O^+; \quad pK_a\,(25°C) = 6.37 \qquad (1)$$

the control and constant monitoring of the residual C_i levels in sample suspension after the "mild" CO_2/HCO_3^--depletion procedure and during the FIOPs measurements must be an integral part of all relevant experiments. This is evident from a recent report, where we clearly demonstrated that after a thorough removal of C_i from the buffer solution by bubbling with CO_2-free argon, CO_2 diffused back into the depleted solution within tens of seconds during the transfer of the sample onto the Joliot-type electrode (Shevela et al. 2007). Thus, while our C_i-depletion procedure led to ~50-fold reduction of C_i level in the freshly-depleted medium, the actual level of C_i in sample suspension during the FIOPs measurements (even after short sample handling) rose to ~fivefold below ambient. Such underestimation of the actual C_i level during the experiment may be one of the reasons for the discrepancies in interpretation of the "bicarbonate effect" on the PSII donor side in the literature (Stemler 2002; Van Rensen and Klimov 2005; McConnell et al. 2012; Shevela et al. 2012).

In this study, we have performed FIOPs experiments using a Joliot-type electrode at ambient and at 20-times reduced levels of C_i. To achieve and maintain such low level of C_i in both gas spaces around the electrode and aqueous phase around the sample, the FIOPs measurements were done inside a glove-box filled with N_2 and in C_i-depleted buffers. In our present FIOPs experiments, we have fully controlled the levels of the residual C_i upon CO_2/HCO_3^--depletion procedure. Thus, the concentration of CO_2 in the gas phase above the sample was continuously monitored with an infrared CO_2 analyzer, while C_i levels in sample suspensions were detected by membrane-inlet mass spectrometry (MIMS).

Materials and methods

Sample preparation

Thylakoids were prepared from fresh leaves of *Spinacia oleracea* based on methods described earlier (Winget et al. 1965) with slight modifications (Messinger et al. 1997). The rates of O_2 evolution for such thylakoid preparations were ~270 µmol (O_2) × mg (Chl)$^{-1}$ × h^{-1}. After isolation steps the thylakoids were frozen in small aliquots in liquid nitrogen and then stored at −80 °C until used. Shortly before measurements, the samples were thawed in the dark on ice and diluted to desired concentrations with "SNM buffer" (400 mM sucrose, 35 mM NaCl, and 20–40 mM MES/KOH) adjusted to pH 6.3.

CO_2/HCO_3^--depletion and monitoring of C_i levels

Depletion of C_i from media and spinach thylakoids was achieved as described earlier (Shevela et al. 2007) with some modifications: initially, C_i was removed from the SNM buffer by means of 60 min flushing with N_2 depleted of CO_2 by passage through a 20-cm layer of ascarite (5–20 mesh particle size; Sigma-Aldrich, Seelze, Germany). This resulted in our C_i-depleted (C_i^-) media. To avoid contamination of C_i^- media with atmospheric CO_2, the depletion procedure and all following sample handling and measuring steps were performed inside a glove-box ("Belle") that was filled with a slight overpressure of N_2. The level of CO_2 inside the glove-box was constantly monitored by The Qubit Systems IRGA CO_2 Analyzer (Model No. S151). To reduce the amount of CO_2 in the N_2 flow, the incoming house N_2 (liquid N_2 blow off) was passed through a 20-cm ascarite-column (see above) before it entered the glove-box. The final CO_2 concentration inside the glove-box after such depletion procedure was in the range of 10–20 ppm (C_i^- conditions), while the CO_2 level off the air was about 390 ppm (C_i^+ conditions).

Thylakoids were depleted of C_i by 20–25-fold dilution with the C_i^- medium and subsequent dark-incubations on ice for 10−20 min. Thereafter, the samples were collected by centrifugation and washed at least twice in the C_i^- medium resulting in the C_i^- samples. Prior to the FIOPs measurements, the sample pellet was diluted with the C_i^- medium to a Chl concentration of 1 mg ml^{-1}.

FIOPs measurements

After long-term (several months) dark low-temperature sample storage, the preparations are enriched (≥80 %) in the reduced form of tyrosine D (Y_D) (Messinger and Renger 1990; Vass et al. 1990b). In order to populate thylakoids with oxidized form of Y_D (Y_D^{ox}), all samples were pre-flashed with one saturating flash and subsequently incubated in darkness for 5 min shortly before the FIOPs measurements.

FIOPs measurements were carried out within a Belle glove-box either under the C_i^+ conditions, when the samples were incubated and measured in the C_i^+ medium (that contained a mixture of CO_2 and HCO_3^-) with open glove-box, or under the C_i^- conditions, in which the samples were incubated and measured in the C_i^- medium under C_i-depleted N_2 atmosphere as described above.

The FIOPs were obtained in the absence of exogenous electron acceptors with a home-built Joliot-type bare Pt-electrode (Joliot 1972; Messinger 1993). The measurements were performed at an electrode temperature of 20 °C (±0.3 °C). To insure complete sedimentation and temperature equilibration, the sample aliquots (10 µl) were kept for 3 min on the Pt-electrode prior to starting the measurements. The polarization voltage (−750 mV) was switched on 40 s before exposure of the samples to a train of saturating Xenon flashes (given by Perkin Elmer, LS-1130-4) at a frequency of 2 Hz. The amplified amperometric signals were recorded with a personal computer at a sampling rate of 3 ms/point. For the C_i^- conditions, only freshly prepared C_i^- buffer (SNM, pH 6.3) was used as a flow medium. For details on a setup of a Joliot-type electrode, see Messinger (1993) and Renger and Hanssum (2009).

FIOPs analysis

The FIOPs were analyzed using a spread sheet program that is based on an extended Kok model (see Fig. 1b) which was described earlier (Isgandarova et al. 2003; Nöring et al. 2008). In addition to the normal Kok parameters, the program included a correction factor (*d*) for a change of the number of active O_2-evolving centers during the flash train (Messinger et al. 1997). Since no agreement has yet been reached about the precise S_i state dependence of the miss parameter, all FIOPs were analyzed employing the equal miss and *two* possible S_i state-dependent miss fitting approaches. For these latter approaches, the S_i state-dependent miss parameters (α_{12}, α_{23}, α_{30}, α_{01}; see Fig. 1b) were allowed to vary (for further details on the S_i state-dependent miss factors, see de Wijn and van Gorkom 2002; Shinkarev 2005; Messinger and Renger 2008; Renger and Hanssum 2009; Han et al. 2012; and Suzuki et al. 2012). However, using all these miss parameters as free variables leads to an underdetermined fit due to the limited number of independent data points in a single FIOP. Therefore, in one case the α-values for the transitions $S_0 \rightarrow S_1$ and $S_1 \rightarrow S_2$ were fixed to "0" ($\alpha_{01} = \alpha_{12} = 0$) since they are assumed to be significantly smaller than those of $S_2 \rightarrow S_3$ and $S_3 \rightarrow S_0 + O_2 + nH^+$ transitions, which were used as free running parameters, but fixed to be equal, i.e., $\alpha_{23} = \alpha_{30}$. This fit approach, which was successfully applied by us previously (Isgandarova et al. 2003), is an extreme form of the parameters suggested by de Wijn and van Gorkom (2002) and Suzuki et al. (2012). In the second unequal miss fit approach, the FIOPs were analyzed assuming high miss probabilities for the $S_0 \rightarrow S_1$, $S_1 \rightarrow S_2$, and $S_2 \rightarrow S_3$ transitions, and almost none for the $S_3 \rightarrow S_0$ transition, as was proposed recently by Han et al. (2012). In such fits, the α_{01}, α_{12}, and α_{23} values were set as free, but equal, running parameters (i.e., $\alpha_{01} = \alpha_{12} = \alpha_{23}$), while the α_{30} was fixed to "0". The comparison of the three approaches should therefore allow evaluating if the fit results are stable toward various possible models for the fitting. The values of 100 % S_1 state and 0 % Y_D populations were fixed for all fits, since we employed pre-flashed samples and because fits in which the dark S-state populations were varied did not yield any significant S_2 or S_0 populations.

Membrane-inlet mass spectrometry measurements

The content of C_i (HCO_3^-/CO_2) in the C_i^- and C_i^+ working buffers (pH 6.3) was measured by membrane-inlet mass spectrometry (MIMS) (Konermann et al. 2008; Beckmann et al. 2009) according to the procedure described previously (Shevela et al. 2007). MIMS measurements were performed by an isotope ratio mass spectrometer (ThermoFinnigan^{Plus} XP) that was connected via a cooling trap (dry ice+C_2H_5OH; ~200 K) to a home-built membrane-inlet cell very similar to that described earlier (Messinger et al. 1995). The working volume of the chamber (150 µl) was separated from a high vacuum (3×10^{-8} bar) of the mass spectrometer via an inlet (Ø 10 mm) that was covered by a 25 µm-thick silicon membrane (Mempro MEM-213) resting on a porous Teflon support (Small Parts Inc.) and permeable only for gasses. Before the measurements, the SNM buffer (pH 6.3) in the measuring chamber was degassed for 20–30 min until an only slightly sloping baseline was reached. After that, 5 µl aliquots of buffer solutions were injected into the chamber. To avoid CO_2 contamination from air when handling samples, all transfers into membrane-inlet chamber were made within 20 s with gas-tight syringes that were pre-flushed with argon. The reaction mixture was constantly kept at 20 °C and stirred with a magnetic stir bar. CO_2 was monitored online at *m*/*z* 44. CO_2 levels in the media were obtained by determining the area under the *m*/*z* 44 signal using OriginPro software.

Results

Monitoring the C_i levels in C_i^- and C_i^+ buffers

Monitoring the actual levels of C_i in working media under each C_i^- and C_i^+ experimental conditions is highly important when studying effects of C_i on PSII. Figure 2 displays the levels of CO_2 in the C_i^+ buffers (trace *1*) and in C_i^- buffer (trace *2*) at pH 6.3 and 20 °C, as monitored by MIMS. A comparison of these two traces shows that our C_i depletion procedure (see "Materials and methods" section) significantly reduces the level of CO_2 in the medium. It is also evident from trace *3* in Fig. 2 that the level of CO_2 in the C_i^- buffer remains almost at the same level even after 2-h-storage under CO_2-depleted N_2 atmosphere inside the glovebox. Analysis of the area of CO_2 signals shows that our set-up

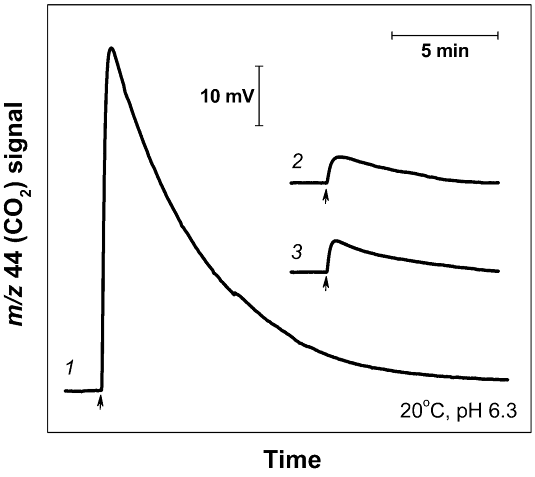

Fig. 2 MIMS measurements of the C_i content in working media used in this study. 5 µl aliquots each were injected into MNS buffer (pH 6.3) that was thoroughly degassed in the 150-µl MIMS cell at 20 °C. The time of injection is marked by *arrows*. Samples: MNS buffer (pH 6.3) before (trace *1*) and after (trace *2*) C_i-depletion by N_2-gas-stream that was also used for filling in atmosphere inside the glove-box (for details see "Materials and methods" section). Trace *3* is the same as trace *2*, but after 2-h exposure of the C_i-depleted buffer to the N_2-gas atmosphere inside the glove-box

allowed measurements of FIOPs at about 20-fold reduced C_i levels in the media as compared to the level of C_i under ambient air conditions. The C_i depletion factor of 20 in sample solution correlates very well with the factor of reduction of CO_2 concentration in the gas phase above the sample (from 390 ppm CO_2 in air to the maximal concentration of 20 ppm CO_2 in CO_2-depleted N_2 atmosphere).

FIOPs experiments

Figure 3 displays normalized FIOPs (symbols) of spinach $S_1Y_D^{ox}$ thylakoids that were obtained at pH 6.3 at two C_i levels. The FIOP shown in Fig. 3a was obtained in the C_i^+ sample under ambient conditions (390 ppm CO_2 in air). It exhibits a typical period-four oscillation with maxima at the 3rd, 7th, 11th, and 15th flashes (see insert for original polarographic signal). For quantification of the obtained FIOPs we analyzed them by three different approaches within the "extended" Kok model (see Fig. 1b and "Materials and methods" section). The results are summarized in Table 1.

In the most simple and widely used fit approach (fits a_1–a_3), the misses (α) and double hits (β) were assumed to be equal in each S_i transition. In such a case, the Kok parameters ($\alpha = 9.1$ % and $\beta = 2.8$ %) in the C_i^+ samples are typical for spinach thylakoids illuminated with Xenon flashes (Hillier and Messinger 2005; Messinger and Renger 2008). However, there are convincing arguments that the miss parameter is S_i state dependent. The reason for using S_i state independent miss parameter is that a single FIOP does not contain enough independent data points to uniquely extract the S_i state dependence of the miss factor. EPR and FTIR spectroscopy were recently employed to study the S_i state dependence of the miss parameter, but two quite different results were obtained (Han et al. 2012; Suzuki et al. 2012). To insure that any possible differences in the miss parameter between C_i^+ and C_i^- samples are not fit model dependent, we employ here two simplified extreme cases of the above suggestions to fit our data.

A good improvement of the fit quality (*Fq*) can be achieved with a fit approach, in which the α-values for the transitions $S_0 \rightarrow S_1$ and $S_1 \rightarrow S_2$ are set to be "zero," while those for the transitions $S_2 \rightarrow S_3$ and $S_3 \rightarrow (S_4) \rightarrow S_0$ are free running parameters that are forced to be equal (Isgandarova et al. 2003; Shevela et al. 2006a; Nöring et al. 2008) (also see "Materials and methods" section). This approach is an extreme case of the S state dependence described by Suzuki et al. (2012) based on FTIR data. The results derived from such approach are shown as fits b_1–b_3 in Table 1 and are depicted for each FIOP as solid lines in Fig. 3. With this fit approach, the α-value in the C_i^+ sample was found to be 15.5 % for the two terminal S_i state transitions, and double hits had a value of 2.5 %. Based on the obtained *Fq* values for fits *a* and *b* (smaller values indicate a better fit), we conclude that although all both fit approaches allow a good description of the data, the unequal miss fit approach *b* provides a slightly better description of the data. As the third fit approach (see fits c_1–c_3 in Table 1), we employ a simplified version of the S_i state dependence of the miss parameter reported by Han et al. (2012). These authors found that at 20 °C the miss parameter is between 10 and 16 % for the $S_0 \rightarrow S_1$, $S_1 \rightarrow S_2$, and $S_2 \rightarrow S_3$ transitions, and very small (3 %) for the $S_3 \rightarrow S_0$ transition. To minimize the number of free variables we therefore forced α_{01}, α_{12} and α_{23} to be equal and varied them together, while α_{30} was fixed to 0 %. The results of this fit approach confirm (with worse *Fq* values) the above-described analysis performed by fits *a* and *b*.

To evaluate the effect of C_i depletion, the above data obtained in C_i^+ samples (Fig. 3a) were compared with normalized FIOPs of the C_i^- samples (see Fig. 3b) that were obtained under C_i-depleted conditions (i.e., 10–20 ppm CO_2 in a glove-box atmosphere). A close comparison of the data reveals that FIOPs of the C_i^- samples have reproducibly a higher damping as compared to that observed in the C_i^+ thylakoids (for a better visualization, gray symbols and dashed line in Fig. 3b represent FIOP of the C_i^+ sample, i.e., the same as in Fig. 3a). Detailed FIOPs analysis confirms these qualitative observations, independent of which fit approach was used (Table 1). According to all three fit approaches, the average miss parameter in the C_i^- samples reproducibly increases by about 2–3 % as compared to the α-values found in the C_i^+ samples ($p < 0.01$ according to the

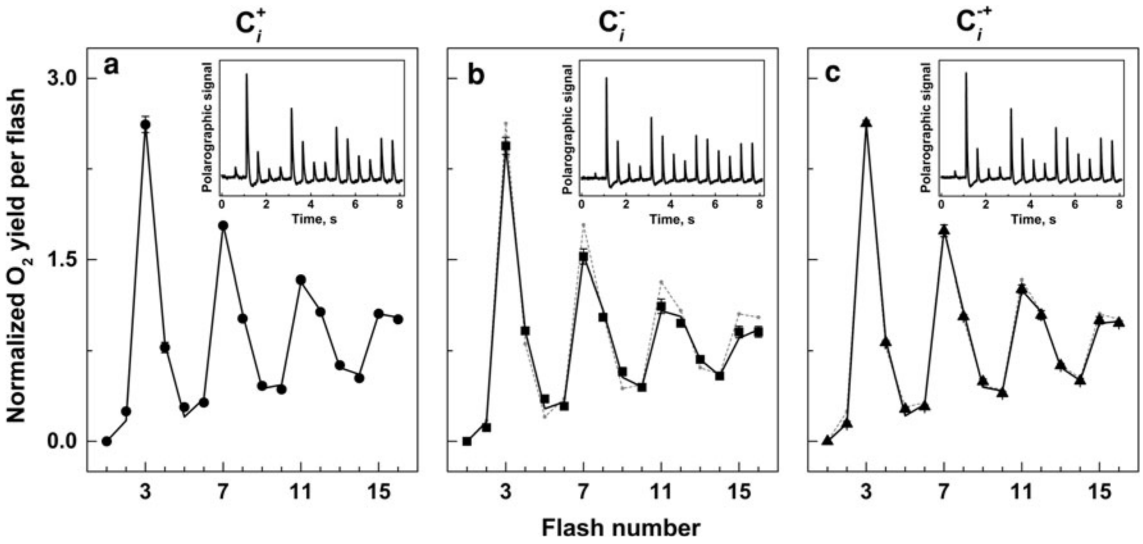

Fig. 3 Normalized FIOPs of dark-adapted thylakoids ($S_1Y_D^{ox}$) from spinach measured under various levels of C_i at pH 6.3. The FIOPs were obtained either in the C_i^+ samples under ambient C_i level (**a**) or in the C_i^- samples under C_i-depleted conditions (**b**). **c** represents FIOP that was monitored in the C_i^{-+} samples that were obtained after addition of 5 mM $NaHCO_3$ to the C_i^- samples. *Solid lines* correspond to the average fits *b* shown in Table 1, while the *symbols* represent the average of experimental values of the collected FIOPs data, and *error bars* show the standard deviations for these values ($n \geq 3$). For a better comparison, *dashed gray lines* and *symbols* in **b** and **c** depict FIOPs of the C_i^+ sample (the same as in **a**). Normalization of the FIOPs was performed by dividing each yield of O_2 per flash by the average of the O_2-yields induced by flashes 3–6 (one cycle). The *insets* show examples of original FIOPs that were recorded with a flash frequency of 2 Hz at 20 °C. No artificial electron acceptors were used

Table 1 Fits of the FIOPs of the $S_1Y_D^{ox}$ thylakoids isolated from spinach and measured at pH 6.3 and 20 °C under various C_i levels (see Fig. 3)

Samples	Fit parameters (%)						$Fq \times 10^{-6}$
	Fits	α_{01}	α_{12}	α_{23}	α_{30}	β	
FIOP C_i^+	a_1	9.1 (0.3)	9.1 (0.3)	9.1 (0.3)	9.1 (0.3)	2.8 (0.1)	19.7 (5.3)
	b_1	0*	0*	15.5 (0.4)	15.5 (0.4)	2.5 (0.1)	10.2 (0.0)
	c_1	12.7 (0.4)	12.7 (0.4)	12.7 (0.4)	0*	2.8 (0.2)	31.2 (9.8)
FIOP C_i^-	a_2	11.4 (0.7)	11.4 (0.7)	11.4 (0.7)	11.4 (0.7)	2.8 (0.2)	31.4 (5.7)
	b_2	0*	0*	19.1 (1.1)	19.1 (1.1)	2.3 (0.2)	13.0 (4.1)
	c_2	15.9 (1.0)	15.9 (1.0)	15.9 (1.0)	0*	2.7 (0.2)	47.4 (7.1)
FIOP C_i^{-+}	a_3	9.6 (0.2)	9.6 (0.2)	9.6 (0.2)	9.6 (0.2)	2.4 (0.1)	17.3 (4.4)
	b_3	0*	0*	16.2 (0.2)	16.2 (0.2)	2.1 (0.1)	6.0 (2.7)
	c_3	13.2 (0.2)	13.2 (0.2)	13.2 (0.2)	0*	2.4 (0.1)	28.1 (5.7)

FIOP C_i^+ was obtained under the ambient (air-saturated) C_i level, while FIOP C_i^- was obtained under the C_i-depleted level. FIOP C_i^{-+} is the same as C_i^-, but after the addition of 5 mM $NaHCO_3$

The FIOPs were fit applying three different approaches, denoted *a*, *b*, and *c* fits. For fits *a* the Kok model with S_i state-independent miss (α) and double-hit (β) parameters was used (for details, see "Introduction" section and "Materials and methods" section). For fits *b* an extended Kok model with S_i state-dependent miss parameters was applied. Thus, the miss parameters of the $S_2 \rightarrow S_3$ and $S_3 \rightarrow S_0$ transitions (α_{23} and α_{30}, respectively) were used as free parameters (but kept equal, i.e., $\alpha_{23} = \alpha_{30}$), while those for the $S_0 \rightarrow S_1$ and $S_1 \rightarrow S_2$ transitions (α_{01} and α_{12}, respectively) were fixed to 0 (marked by asterisk). In fits *c*, the FIOPs were analyzed applying an extended Kok model also with S_i state-dependent misses, where the α-values for the $S_0 \rightarrow S_1$, $S_1 \rightarrow S_2$, and $S_2 \rightarrow S_3$ transitions were rerunning as free parameters, but kept to be equal (i.e., $\alpha_{01} = \alpha_{12} = \alpha_{23}$), while the one for the $S_3 \rightarrow S_0$ transition was fixed to 0. The values of 100 % S_1 state and 0 % Y_D populations were set into the fits. In order to compare fits with different numbers of free parameters, the fit quality (Fq) was calculated according to the following equation: $Fq = \sum dy_n^2/(F - P)$, where $\sum dy_n^2$ is the sum of the squared differences between the fit and the data that was minimized by the program during fits (for further details and full expression, see Isgandarova et al. 2003), F is the number of analyzed flashes (16 in the present study), and P is the number of free parameters used in the fit. The smaller Fq values indicate a better fit. All values are the average of replicate experiments on the same thylakoid preparation that were fit independently, and the numbers in parentheses show the standard deviation ($n \geq 3$)

two-tailed *t* test with an assumption of unequal variance). In order to check the reversibility of the observed effect, we measured the FIOPs shortly (within ∼3 min) after addition of 5 mM HCO_3^- to the C_i^- samples (C_i^{-+} samples). The FIOP shown in Fig. 3c and its fits (Table 1) demonstrate that such addition largely reverses the increase of the miss parameter (the two-tailed, unpaired *t* test for the C_i^- and C_i^{-+} samples; $p < 0.01$). Interestingly, the double hits were found to be almost identical in the C_i^- and C_i^+ samples, and only insignificantly decreased in the C_i^{-+} samples. While the data presented in the manuscript were obtained with one specific thylakoid preparation, we performed test experiments with other preparations and consistently found a similar increase of the miss parameter after C_i-depletion.

Thus, the above presented FIOPs data and the numerical analysis clearly show that a 20-fold reduction of the C_i level in the sample medium decreases the PSII turnover efficiency (i.e., increases the miss parameter) in spinach thylakoids, while the addition of HCO_3^- to C_i-depleted samples largely restores it.

Discussion

The results obtained in this FIOPs study clearly demonstrate a small, but reproducible increase of misses at strongly reduced C_i levels in sample suspension and in the gas phase above the sample as compared to the ambient levels of C_i in the air-exposed conditions. In previous FIOPs studies that employed a similar C_i depletion method for thylakoids, no change of the miss-values were found (Shevela et al. 2006b, 2007) unless formate or acetate were added to replace HCO_3^- from PSII (Stemler et al. 1974; Mende and Wiessner 1985; Shevela et al. 2007). This discrepancy can be readily explained by the relatively high residual level of C_i in the C_i^- samples during the FIOPs measurements in these previous studies. Thus, in our previous report we showed, that during sample transfer onto the Joliot-type electrode and its subsequent polarization (∼40 s) required for the FIOPs measurements, the initial 50-fold reduction of the C_i level in the freshly-depleted sample solution rises to about fivefold below ambient at the time of the FIOPs measurements (Shevela et al. 2007). This happens due to the fairly quick diffusion of CO_2 from air back to the C_i^- sample suspension. In the present study, we excluded contamination of CO_2 from air by performing C_i-depletion, transfers and measuring procedures inside the glove-box flushed in with N_2 that contained maximum 20 ppm CO_2. This experimental design allowed us to obtain FIOPs at 4-times lower levels of C_i than in earlier report (20-fold vs. ∼fivefold depletion). This clearly demonstrates that, in addition to the C_i-depletion method, the actual levels of CO_2/HCO_3^- in the investigated samples are highly important and must be monitored in any relevant studies of HCO_3^- effects in PSII. In principle, it is possible that the anaerobic conditions during measurements of the C_i^- thylakoids contribute to the observed increase of the miss parameter. However, HCO_3^- addition under anaerobic conditions largely reversed the miss factor back to normal (Fig. 3). We therefore conclude that the possible contribution of O_2-free conditions is negligible.

It is known that the misses may reflect the properties of both the donor and the acceptor side of PSII (Messinger et al. 1993; Shinkarev and Wraight 1993). The increased magnitude of the α-values at C_i^- conditions may therefore either indicate (i) changes in redox equilibria between the donor and the acceptor side of PSII (i.e., redox-potential differences between $Q_B^{\bullet-}Q_A/Q_BQ_A^{\bullet-}$, $P680/P680^{\bullet+}$, Y_Z/Y_Z^{ox} and the S_i states of the OEC) (Renger and Hanssum 1988; Shinkarev and Wraight 1993), (ii) the slower reduction of $P680^{\bullet+}$ by Y_Z (Christen et al. 1999), or (iii) slowed proton release from the OEC during water-splitting (Zaharieva et al. 2011). While the misses may reflect the properties of both the donor and the acceptor side of PSII, the double hits reflect mainly the properties of the acceptor side and are related linearly to the rate of electron transfer from $Q_A^{\bullet-}$ to $Q_B/Q_B^{\bullet-}$ (Messinger et al. 1993). Giving the fact that the β-values were found to be almost unaffected (Table 1) by the removal of CO_2/HCO_3^- in the samples, the changes in misses most likely appears to be restricted to events on the donor side of PSII (i.e., to the OEC).

Evidence for the role of "bicarbonate" to regulate the electron transfer on the acceptor side of PSII has been established in numerous previous studies (for recent reviews, see Van Rensen 2002; Van Rensen and Klimov 2005; McConnell et al. 2012; Shevela et al. 2012). It was shown to be bound to the non-heme iron (NHI) located between Q_A and Q_B (Diner and Petrouleas 1990; Hienerwadel and Berthomieu 1995), and this binding has been recently supported by PSII crystal structures (Guskov et al. 2010; Umena et al. 2011). Current model suggests that HCO_3^-/CO_3^{2-} facilitates the reduction of Q_B and participates in its protonation involving the H-network of D1-H215 and other residues (Berthomieu and Hienerwadel 2001; Cox et al. 2009; Cardona et al. 2012; Müh et al. 2012; Shevela et al. 2012; Saito et al. 2013). This acceptor side "bicarbonate" is known to be a so tightly bound ligand to the NHI that it can be efficiently exchanged/removed only by high concentrations of other carboxylic acids, such as formate or acetate (Govindjee et al. 1991, 1997; Aoyama et al. 2008; Shevela et al. 2008a, b; Ulas et al. 2008). In the present study, no formate or acetate was added to the sample during C_i-depletion procedure. It is therefore very unlikely that the observed effect of low CO_2/HCO_3^- levels in the sample suspension on the misses originates from the electron-acceptor side "bicarbonate".

El-Shintinawy and Govindjee (1990) found with spinach leaf disks that HCO_3^--depletion resulted in an about 40 % loss of the O_2-evolving activity after a short (10 s) infiltration of the leaf disks in C_i-free media that did not contain formate (and acetate) as compared to un-infiltrated (control) samples. Based on the observation that only 15 % of the O_2 evolution rate was impaired after the same infiltration procedure, but in the presence of exogenous HCO_3^-, the authors concluded that the observed effect was caused not only by the infiltration procedure, but also due to a partial C_i depletion of the leaf disks (El-Shintinawy and Govindjee 1990). These results are in a good agreement with the effects of formate/acetate-free C_i-depletion on miss parameter found in our study. It should be mentioned, that similar depletion procedure via infiltration of the leaf disks in the presence of formate induced the "bicarbonate effect," and thereby gave an indication for two sites of action for the HCO_3^- (one beyond Q_A, and another one was speculated to be between the primary electron acceptor, pheophytin, and Q_A) (El-Shintinawy and Govindjee 1990).

In contrast to the acceptor side effect, the role of HCO_3^- ions in the process of water oxidation on the electron-donor side of PSII is not well understood (Stemler 2002; Van Rensen and Klimov 2005; Shevela et al. 2012). Several hypotheses for its functioning within (or in the vicinity of) the OEC were/are currently discussed: (i) exchangeable HCO_3^- supplies substrate H_2O to the OEC (Warburg 1964; Metzner 1978); (ii) tightly bound non-exchangeable HCO_3^- is a structural part of the functional Mn_4CaO_5 cluster (Allakhverdiev et al. 1997; Klimov et al. 1997; Ferreira et al. 2004); (iii) HCO_3^- is a native cofactor during photo-assembly of the Mn_4CaO_5 cluster, but is not part of the functioning OEC (Baranov et al. 2000, 2004) and (iv) a loosely bound (or non-bound) exchangeable HCO_3^- is involved in proton removal during photosynthetic water oxidation (Villarejo et al. 2002; Ananyev et al. 2005). The results obtained by many laboratories have made the two first hypotheses very unlikely (Clausen et al. 2005; Hillier et al. 2006; Siegbahn and Lundberg 2006; Aoyama et al. 2008; Shevela et al. 2008b; Ulas et al. 2008; Guskov et al. 2010; Umena et al. 2011), while the role of HCO_3^- during photoactivation of the OEC was confirmed by recent EPR data (Dasgupta et al. 2007, 2008, 2010). Recently, the first indications for participation of HCO_3^- in removal of protons from the OEC were reported (Shutova et al. 2008; Ulas and Brudvig 2010). In particular, Shutova et al. (2008) showed that in algae *Chlamydomonas reinhardtii*, HCO_3^- and Cah3 protein (the carbonic anhydrase protein associated with the PSII donor side in *C. reinhardtii*) have "donor side" effects only on proton release steps, and not on the electron transfer steps. Ulas and Brudvig (2010), using exogenous zwitterion (glycine betaine) as selective inhibitors of proton-transport processes, showed that the decreased catalytic rate of the OEC in *Synechocystis* PCC 6803 is recovered upon addition of exogenous HCO_3^-. Our FIOPs data presented here are in a good agreement with these results and thus with the idea that HCO_3^- may be required for the efficient turnover of the OEC by facilitating the proton release away from the OEC during water-splitting. Indeed, de-protonation reactions of the OEC are thought to have a significant impact on the thermodynamics of water oxidation (for reviews, see Krishtalik 2000 and Dau and Haumann 2008). Zaharieva et al. (2011) showed that high proton concentration in the vicinity of Mn_4CaO_5 cluster can severely inhibit the light-induced S_i state transitions of the Kok cycle. Such inhibition should be reflected as increased overall miss factor of the Kok cycle. Therefore, an increase of the miss factor in our C_i-depleted samples may be indicative for less effective de-protonation of the OEC due to a deficit of HCO_3^- species. The observation of the partial restoration of the turnover efficiency of the OEC upon the addition of the extrinsic HCO_3^- to the C_i^- samples is completely coherent with this suggestion.

Acknowledgments This study was supported by the *Knut and Alice Wallenberg Foundation*, the *Kempe Foundation*, the *Swedish Research Council (VR)*, the *Strong Research Environment Solar Fuels* (Umeå University), the *Artificial Leaf Project* (K&A Wallenberg Foundation) and *the Max-Planck Gesellschaft*. The authors would like to thank Govindjee, Vyacheslav Klimov, and Alan Stemler for fruitful discussions on the "bicarbonate effect" over the last few years and Ethel Hüttel for sample preparation.

References

Allakhverdiev SI, Yruela I, Picorel R, Klimov VV (1997) Bicarbonate is an essential constituent of the water-oxidizing complex of photosystem II. Proc Natl Acad Sci USA 94(10):5050–5054

Ananyev G, Dismukes GC (2005) How fast can photosystem II split water? Kinetic performance at high and low frequencies. Photosynth Res 84(1):355–365

Ananyev G, Nguyen T, Putnam-Evans C, Dismukes GC (2005) Mutagenesis of CP43-arginine-357 to serine reveals new evidence for (bi)carbonate functioning in the water oxidizing complex of photosystem II. Photochem Photobiol Sci 4(12):991–998

Aoyama C, Suzuki H, Sugiura M, Noguchi T (2008) Flash-induced FT-IR difference spectroscopy shows no evidence for the structural coupling of bicarbonate to the oxygen-evolving Mn cluster in photosystem II. Biochemistry 47(9):2760–2765

Baranov SV, Ananyev GM, Klimov VV, Dismukes GC (2000) Bicarbonate accelerates assembly of the inorganic core of the water-oxidizing complex in manganese depleted photosystem II: a proposed biogeochemical role for atmospheric carbon dioxide in oxygenic photosynthesis. Biochemistry 39(20):6060–6065

Baranov SV, Tyryshkin AM, Katz D, Dismukes GC, Ananyev GM, Klimov VV (2004) Bicarbonate is a native cofactor for assembly of the manganese cluster of the photosynthetic water oxidizing complex. Kinetics of reconstitution of O_2 evolution by photoactivation. Biochemistry 43(7):2070–2079

Beckmann K, Messinger J, Badger MR, Wydrzynski T, Hillier W (2009) On-line mass spectrometry: membrane inlet sampling. Photosynth Res 102:511–522

Berthomieu C, Hienerwadel R (2001) Iron coordination in photosystem II: interaction between bicarbonate and Q_B pocket studied by Fourier transform infrared spectroscopy. Biochemistry 40:4044–4052

Cardona T, Sedoud A, Cox N, Rutherford AW (2012) Charge separation in Photosystem II: a comparative and evolutionary overview. Biochim Biophys Acta 1817(1):26–43

Christen G, Seeliger A, Renger G (1999) $P680^{+\cdot}$ reduction kinetics and redox transition probability of the water oxidizing complex as a function of pH and H/D isotope exchange in spinach thylakoids. Biochemistry 38(19):6082–6092

Clausen J, Beckmann K, Junge W, Messinger J (2005) Evidence that bicarbonate is not the substrate in photosynthetic oxygen evolution. Plant Physiol 139(3):1444–1450

Cox N, Messinger J (2013) Reflections on substrate water and dioxygen formation. Biochim Biophys Acta. doi:10.1016/j.bbabio.2013.01.013 (in press)

Cox N, Jin L, Jaszewski A, Smith PJ, Krausz E, Rutherford AW, Pace R (2009) The semiquinone-iron complex of photosystem II: structural insights from ESR and theoretical simulation; evidence that the native ligand to the non-heme iron is carbonate. Biophys J 97(7):2024–2033

Dasgupta J, Tyryshkin AM, Dismukes GC (2007) ESEEM spectroscopy reveals carbonate and an N-donor protein-ligand binding to Mn^{2+} in the photoassembly reaction of the Mn_4Ca cluster in photosystem II. Angew Chem Int Ed 46(42):8028–8031

Dasgupta J, Ananyev GM, Dismukes GC (2008) Photoassembly of the water-oxidizing complex in photosystem II. Coord Chem Rev 252(3–4):347–360

Dasgupta J, Tyryshkin AM, Baranov SV, Dismukes GC (2010) Bicarbonate coordinates to Mn^{3+} during photo-assembly of the catalytic Mn_4Ca core of photosynthetic water oxidation: EPR characterization. Appl Magn Reson 37(1–4):137–150

Dau H, Haumann M (2008) The manganese complex of photosystem II in its reaction cycle: basic framework and possible realization at the atomic level. Coord Chem Rev 252(3–4):273–295

Dau H, Zaharieva I, Haumann M (2012) Recent developments in research on water oxidation by photosystem II. Curr Opin Chem Biol 16(1–2):3–10

de Wijn R, van Gorkom HJ (2002) S-state dependence of the miss probability in photosystem II. Photosynth Res 72(2):217–222

Diner BA (1977) Dependence of deactivation reactions of photosystem II on redox state of plastoquinone pool A varied under anaerobic conditions. Equilibria on the acceptor side of photosystem II. Biochim Biophys Acta 460:247–258

Diner BA, Petrouleas V (1990) Formation by NO of nitrosyl adducts of redox components of the photosystem II reaction center. 2. Evidence that HCO_3^-/CO_2 binds to the acceptor-side non-heme iron. Biochim Biophys Acta 1015(1):141–149

El-Shintinawy F, Govindjee (1990) Bicarbonate effect in leaf discs from spinach. Photosynth Res 24:189–200

Ferreira KN, Iverson TM, Maghlaoui K, Barber J, Iwata S (2004) Architecture of the photosynthetic oxygen-evolving center. Science 303(5665):1831–1838

Forbush B, Kok B, McGloin MP (1971) Cooperation of charges in photosynthetic oxygen evolution. II. Damping of flash yield oscillation, deactivation. Photochem Photobiol 14(3):307–321

Fromme R, Hagemann R, Renger G (1987) Comparative studies of electron transport and atrazine binding in thylakoids and PS II particles from spinach. In: Biggens J (ed) Progress in Photosynthesis Research, vol III. Martinus Nijhoff Publishers, Dordrecht, pp 783–786

Govindjee, Xu C, van Rensen JJS (1997) On the requirement of bound bicarbonate for photosystem II activity. Z Naturforsch 52(1–2):24–32

Govindjee Weger HG, Turpin DH, van Rensen JJS, Devos OJ, Snel JFH (1991) Formate releases carbon dioxide/bicarbonate from thylakoid membranes: measurements by mass spectroscopy and infrared gas analyzer. Naturwissenschaften 78(4):168–170

Govindjee, Kern J, Messinger J, Whitmarsh J (2010) Photosystem II. In: Encyclopedia of Life Sciences (ELS). Wiley, Chichester. doi:10.1002/9780470015902.a0000669.pub2

Guskov A, Gabdulkhakov A, Broser M, Glöckner C, Hellmich J, Kern J, Frank M, Saenger W, Zouni A (2010) Recent progress in the crystallographic studies of photosystem II. ChemPhysChem 11:1160–1171

Han GY, Mamedov F, Styring S (2012) Misses during water oxidation in photosystem II are S state-dependent. J Biol Chem 287(16):13422–13429

Hienerwadel R, Berthomieu C (1995) Bicarbonate binding to the non-heme iron of photosystem II investigated by Fourier transform infrared difference spectroscopy and 13C-labeled bicarbonate. Biochemistry 34:16288–16297

Hillier W, Messinger J (2005) Mechanism of photosynthetic oxygen production. In: Wydrzynski T, Satoh K (eds) Photosystem II. The Light-Driven water:plastoquinone oxidoredutase, vol 22. Advances in photosynthesis and respiration. Springer, Dordrecht, pp 567–608

Hillier W, McConnell I, Badger MR, Boussac A, Klimov VV, Dismukes GC, Wydrzynski T (2006) Quantitative assessment of intrinsic carbonic anhydrase activity and the capacity for bicarbonate oxidation in photosystem II. Biochemistry 45(7):2094–2102

Isgandarova S, Renger G, Messinger J (2003) Functional differences of photosystem II from *Synechococcus elongatus* and spinach characterized by flash-induced oxygen evolution patterns. Biochemistry 42(30):8929–8938

Joliot P (1972) Modulated light source use with the oxygen electrode. In: San Pietro A (ed) Photosynthesis and nitrogen fixation, vol 24 B. Methods of enzymology. Academic Press, New York, pp 123–134

Joliot P (2003) Period-four oscillations of the flash-induced oxygen formation in photosynthesis. Photosynth Res 76(1–3):65–72

Joliot P, Barbieri G, Chabaud R (1969) Un nouveau modele des centres photochimiques du systeme II. Photochem Photobiol 10:309–329

Jursinic P (1981) Investigation of double turnovers in photosystem II charge separation and oxygen evolution with excitation flashes of different duration. Biochim Biophys Acta 635:38–52

Jursinic P, Stemler A (1982) A seconds range component of the reoxidation of the primary photosystem II acceptor Q: effects of bicarbonate depletion in chloroplasts. Biochim Biophys Acta 681(3):419–428

Jursinic PA, Stemler A (1984) Effects of bicarbonate depletion on secondary acceptors of photosystem II. Biochim Biophys Acta 764(2):170–178

Kebekus U, Messinger J, Renger G (1995) Structural changes in the water oxidizing complex monitored via the pH dependence of the reduction rate of redox state S_1 by hydrazine and hydroxylamine in isolated spinach thylakoids. Biochemistry 34:6175–6182

Klimov VV, Allakhverdiev SI, Baranov SV, Feyziev YM (1995a) Effects of bicarbonate and formate on the donor side of photosystem 2. Photosynth Res 46(1–2):219–225

Klimov VV, Allakhverdiev SI, Feyziev YM, Baranov SV (1995b) Bicarbonate requirement for the donor side of photosystem II. FEBS Lett 363(3):251–255

Klimov VV, Hulsebosch RJ, Allakhverdiev SI, Wincencjusz H, van Gorkom HJ, Hoff AJ (1997) Bicarbonate may be required for ligation of manganese in the oxygen-evolving complex of photosystem II. Biochemistry 36(51):16277–16281

Kok B, Forbush B, McGloin M (1970) Cooperation of charges in photosynthetic O_2 evolution. Photochem Photobiol 11:457–476

Konermann L, Messinger J, Hillier W (2008) Mass spectrometry based methods for studying kinetics and dynamics in biological systems. In: Amesz J, Hoff AJ (eds) Biophysical techniques in photosynthesis, vol 26., Series advances in photosynthesis and respirationSpringer, Dordrecht, pp 167–190

Kouřil R, Dekker JP, Boekema EJ (2012) Supramolecular organization of photosystem II in green plants. Biochim Biophys Acta 1817(1):2–12

Krishtalik LI (2000) The mechanism of the proton transfer: an outline. Biochim Biophys Acta 1458(1):6–27

Mar T, Govindjee (1972) Kinetic models of oxygen evolution in photosynthesis. J Theoret Biol 36:427–446

McConnell IL, Eaton-Rye JJ, Van Rensen JJS (2012) Regulation of photosystem II electron transport by bicarbonate. In: Eaton-Rye JJ, Tripathy BC, Sharkey TD (eds) Photosynthesis: plastid biology, energy conversion and carbon assimilation. Springer, Dordrecht, pp 475–500

Mende D, Wiessner W (1985) Bicarbonate in vivo requirement of photosystem II in the green alga *Chlamydobotrys stellata*. J Plant Physiol 118(3):259–266

Messinger J (1993) Untersuchungen über die reaktiven Eigenschaften der verschiedenen Redoxzustände der Wasseroxidase Höherer Pflanzen. TU Berlin, Berlin

Messinger J, Renger G (1990) The reactivity of hydrazine with PS II strongly depends on the redox state of the water oxidizing system. FEBS Lett 277:141–146

Messinger J, Renger G (1993) Generation, oxidation by the oxidized form of the tyrosine of polypeptide D2, and possible electronic configuration of the redox States S_0, S_{-1} and S_{-2} of the water oxidase in isolated spinach thylakoids. Biochemistry 32(36):9379–9386

Messinger J, Renger G (2008) Photosynthetic water splitting. In: Renger G (ed) Primary processes of photosynthesis, part 2 principles and apparatus, vol 9., Comprehensive series in photochemical and photobiological sciencesRSC Publishing, Cambridge, pp 291–351

Messinger J, Schröder WP, Renger G (1993) Structure-function relations in photosystem II. Effects of temperature and chaotropic agents on the period four oscillation of flash induced oxygen evolution. Biochemistry 32:7658–7668

Messinger J, Badger MR, Wydrzynski T (1995) Detection of one slowly exchanging substrate water molecule in the S_3 state of photosystem II. Proc Natl Acad Sci USA 92:3209–3213

Messinger J, Seaton G, Wydrzynski T, Wacker U, Renger G (1997) S_{-3} state of the water oxidase in photosystem II. Biochemistry 36:6862–6873

Metzner H (1978) Photosynthetic oxygen evolution. Academic Press, London

Müh F, Glöckner C, Hellmich J, Zouni A (2012) Light-induced quinone reduction in photosystem II. Biochim Biophys Acta 1817(1):44–65

Nöring B, Shevela D, Renger G, Messinger J (2008) Effects of methanol on the S_i-state transitions in photosynthetic water-splitting. Photosynth Res 98:251–260

Nugent JHA, Demetriou C, Lockett CJ (1987) Electron donation in photosystem II. Biochim Biophys Acta 894(3):534–542

Pobeguts OV, Smolova TN, Timoshevsky DS, Klimov VV (2010) Interaction of bicarbonate with the manganese-stabilizing protein of photosystem II. J Photochem Photobiol B 100:30–37

Renger G (2010) The light reactions of photosynthesis. Curr Sci 98:1305–1319

Renger G, Hanssum B (1988) Studies on the deconvolution of flash induced absorption changes into the difference spectra of individual redox steps within the water oxidizing enzyme system. Photosynth Res 16:243–259

Renger G, Hanssum B (2009) Oxygen detection in biological systems. Photosynth Res 102(2–3):487–498

Renger G, Holzwarth AR (2005) Primary electron transfer. In: Wydrzynski TJ, Satoh K (eds) Photosystem II. The light-driven water: plastoquinone oxidoreductase, vol 22. Advances in photosynthesis and respiration. Springer, Dordrecht, pp 139–175

Saito K, Rutherford AW, Ishikita H (2013) Mechanism of proton-coupled quinone reduction in photosystem II. Proc Natl Acad Sci USA 110(3):954–959

Shevela D, Messinger J (2012) Probing the turnover efficiency of photosystem II membrane fragments with different electron acceptors. Biochim Biophys Acta 1817(8):1208–1212

Shevela D, Nöring B, Eckert HJ, Messinger J, Renger G (2006a) Characterization of the water oxidizing complex of photosystem II of the Chl d-containing cyanobacterium Acaryochloris marina via its reactivity towards endogenous electron donors and acceptors. Phys Chem Chem Phys 8(29):3460–3466

Shevela DN, Khorobrykh AA, Klimov VV (2006b) Effect of bicarbonate on the water-oxidizing complex of photosystem II in the super-reduced S-states. Biochim Biophys Acta 1757(4):253–261

Shevela D, Klimov V, Messinger J (2007) Interactions of photosystem II with bicarbonate, formate and acetate. Photosynth Res 94(2–3):247–264

Shevela D, Klimov V, Messinger J (2008a) Formate-induced release of carbon dioxide/hydrogen carbonate from photosystem II. In: Allen JF, Gantt E, Golbeck JH, Osmond B (eds) Photosynthesis. Energy from the Sun. Springer, Glasgow, pp 497–501

Shevela D, Su JH, Klimov V, Messinger J (2008b) Hydrogen carbonate is not a tightly bound constituent of the water-oxidizing complex in photosystem II. Biochim Biophys Acta 1777(6):532–539

Shevela D, Eaton-Rye JJ, Shen J-R, Govindjee (2012) Photosystem II and the unique role of bicarbonate: a historical perspective. Biochim Biophys Acta 1817(8):1134–1151

Shinkarev V (2005) Flash induced oxygen evolution and other oscillatory processes. In: Wydrzynski T, Satoh K (eds) Photosystem II. The light-driven water: plastoquinone oxidoredutase, vol 22. Advances in photosynthesis and respiration. Springer, Dordrecht, pp 539–565

Shinkarev V, Wraight CA (1993) Oxygen evolution in photosynthesis: from unicycle to bicycle. Proc Natl Acad Sci USA 90:1834–1838

Shutova T, Kenneweg H, Buchta J, Nikitina J, Terentyev V, Chernyshov S, Andersson B, Allakhverdiev SI, Klimov VV, Dau H, Junge W, Samuelsson G (2008) The photosystem II-associated Cah3 in Chlamydomonas enhances the O_2 evolution rate by proton removal. EMBO J 27(5):782–791

Siegbahn PEM, Lundberg M (2006) Hydroxide instead of bicarbonate in the structure of the oxygen evolving complex. J Inorg Biochem 100(5–6):1035–1040

Stemler A (1980) Forms of dissolved carbon dioxide required for photosystem II activity in chloroplast membranes. Plant Physiol 65(6):1160–1165

Stemler A (1982) The functional role of bicarbonate in photosynthetic light reaction II. In: Govindjee (ed) Photosynthesis vol II. Academic Press, New York, pp 513–538

Stemler AJ (2002) The bicarbonate effect, oxygen evolution, and the shadow of Otto Warburg. Photosynth Res 73(1–3):177–183

Stemler A, Govindjee (1973) Bicarbonate ion as a critical factor in photosynthetic oxygen evolution. Plant Physiol 52(2):119–123

Stemler AJ, Lavergne J (1997) Evidence that formate destabilizes the S_{-1} state of the oxygen-evolving mechanism in Photosystem II. Photosynth Res 51(2):83–92

Stemler A, Babcock GT, Govindjee (1974) Effect of bicarbonate on photosynthetic oxygen evolution in flashing light in chloroplast fragments. Proc Natl Acad Sci USA 71(12):4679–4683

Styring S, Rutherford AW (1987) In the oxygen evolving complex of photosystem II the S_0 state is oxidized to the S_1 State by Y_D^+ (Signal II_{slow}). Biochemistry 26:2401–2405

Suzuki H, Sugiura M, Noguchi T (2012) Determination of the miss probabilities of individual S-state transitions during photosynthetic water oxidation by monitoring electron flow in photosystem II using FTIR spectroscopy. Biochemistry 51(34):6776–6785

Ulas G, Brudvig GW (2010) Zwitterion modulation of O_2-evolving activity of cyanobacterial photosystem II. Biochemistry 49(37): 8220–8227

Ulas G, Olack G, Brudvig GW (2008) Evidence against bicarbonate bound in the O_2-evolving complex of photosystem II. Biochemistry 47(10):3073–3075

Umena Y, Kawakami K, Shen J-R, Kamiya N (2011) Crystal structure of oxygen-evolving photosystem II at a resolution of 1.9 Å. Nature 473:55–60

Van Rensen JJS (2002) Role of bicarbonate at the acceptor side of photosystem II. Photosynth Res 73(1–3):185–192

Van Rensen JJS, Klimov VV (2005) Bicarbonate interactions. In: Wydrzynski T, Satoh K (eds) Photosystem II. The light-driven water: plastoquinone oxidoreductase, vol 22. Advances in photosynthesis and respiration. Springer, Dordrecht, pp 329–346

Van Rensen JJS, Xu C, Govindjee (1999) Role of bicarbonate in photosystem II, the water-plastoquinone oxido-reductase of plant photosynthesis. Physiol Plant 105:585–592

Vass I, Deak Z, Hideg E (1990a) Charge equilibrium between the water oxidizing complex and the electron donor tyrosine D in photosystem II. Biochim Biophys Acta 1017:63–69

Vass I, Deak Z, Jegerschold C, Styring S (1990b) The accessory electron-donor tyrosine D of photosystem II is slowly reduced in the dark during low-temperature storage of isolated thylakoids. Biochim Biophys Acta 1018(1):41–46

Vermaas WEJ, Renger G, Dohnt G (1984) The reduction of the oxygen evolving system in chloroplasts by thylakoid components. Biochim Biophys Acta 764(2):194–202

Villarejo A, Shutova T, Moskvin O, Forssen M, Klimov VV, Samuelsson G (2002) A photosystem II-associated carbonic anhydrase regulates the efficiency of photosynthetic oxygen evolution. EMBO J 21(8):1930–1938

Warburg O (1964) Prefactory chapter. Annu Rev Biochem 33:1–18

Warburg O, Krippahl G (1958) Hill-Reaktionen. Z Naturforsch B 13(8):509–514

Winget GD, Izawa S, Good NE (1965) Stoichiometry of photophosphorylation. Biochem Biophys Res Commun 21(5):438–441

Wydrzynski T, Govindjee (1975) New site of bicarbonate effect in photosystem II of photosynthesis: evidence from chlorophyll fluorescence transients in spinach-chloroplasts. Biochim Biophys Acta 387(2):403–408

Wydrzynski T, Satoh K (eds) (2005) Photosystem II. The light-driven water: plastoquinone oxidoreductase, vol 22. Advances in photosynthesis and respiration. Springer, Dordrecht

Yano J, Kern J, Sauer K, Latimer MJ, Pushkar Y, Biesiadka J, Loll B, Saenger W, Messinger J, Zouni A, Yachandra VK (2006) Where water is oxidized to dioxygen: structure of the photosynthetic Mn_4Ca cluster. Science 314:821–825

Zaharieva I, Wichmann JM, Dau H (2011) Thermodynamic limitations of photosynthetic water oxidation at high proton concentrations. J Biol Chem 286(20):18222–18228